

## Optical and dielectric properties of SrMoO<sub>4</sub> powders prepared by the combustion synthesis method

S. Vidya<sup>1</sup>, Annamma John<sup>1</sup>, Sam Solomon<sup>2</sup> and J.K. Thomas\*<sup>1</sup>

<sup>1</sup>*Electronic Materials Research Laboratory, Department of Physics, Mar Ivanios College  
Thiruvananthapuram - 695 015, Kerala, India*

<sup>2</sup>*Dielectric Materials Research Laboratory, Department of Physics, St. John's College,  
Kollam - 691306, Kerala, India*

*(Received May 8, 2012, Revised June 29, 2012, Accepted July 22, 2012)*

**Abstract.** In this paper, we report on the obtention of nanocrystalline SrMoO<sub>4</sub> synthesized through modified combustion process. These powders were characterized by X-ray diffraction, Fourier Transform Raman and Infrared Spectroscopy. These studies reveal that the scheelite-type SrMoO<sub>4</sub> crystallizes in tetragonal structure with I41/a (N#88) space group. Transmission electron microscopy image shows that the nanocrystalline SrMoO<sub>4</sub> powders have average size of 18 nm. The optical band gap determined from the UV-V is absorption spectra for the as prepared sample is 3.7 eV. These powders showed a strong green photoluminescence emission. The samples are sintered at a relatively low temperature of 850°C. The morphology of the sintered pellet is studied with scanning electron microscopy. The dielectric constant and loss factor values obtained at 5 MHz for a well sintered SrMoO<sub>4</sub> pellet has been found to be 9.50 and  $7.5 \times 10^{-3}$  respectively. Thus nano SrMoO<sub>4</sub> is a potential candidate for low temperature co-fired ceramics and luminescent applications.

**Keywords:** photoluminescence; combustion synthesis; nanostructures; dielectric; band gap; sintering

---

### 1. Introduction

Molybdates with scheelite-type tetragonal structure belong a family of compounds with interesting structural features and attractive luminescence properties (Sczancoski 2009, 2010). Because of their remarkable physical and chemical properties they found potential applications in fiber optic communication (Yang 2004, Zhang 2005), heterogeneous catalysts (Paski 1988, Zhang 2005), solid-state lasers (Streifer 1973, Zverev 2004, Yu 2011), laser-host materials (Basiev 2000, Marques 2006), scintillation detector (Ishii 1991), optical devices (Harris 1970, Chang 1996) cryogenic detectors for dark matter (Angloher 1994) and microwave applications (Ryu 2005, Choi 2007). Strontium molybdate is a representative scheelite compound, and its central Mo metal ion is coordinated by four O<sup>2-</sup> ions in tetrahedral symmetry ( $T_d$ ), which makes MoO<sub>4</sub><sup>2-</sup> relatively stable. They remain in tetragonal structure within a wide range of temperatures and pressures (Christofilos 1995, Basiev 2000). The quest for materials with such wide range of properties and that can be sintered at low temperature is of keen interest to research world.

---

\*Corresponding author, Ph. D., E-mail: [jkthomasemrl@yahoo.com](mailto:jkthomasemrl@yahoo.com)

The preparation strategy of this material in the form of coarse grained conventional powder and film are widely reported in literatures employing solid-state sintering (Sabharwal 2006), Czochralski method (Zeng 1997, Jia 2004), solvothermal method (Bi 2009), hydrothermal process (Cheng 2005, Sczancoski 2008), cell electrochemical technique (Chen 2007), chemical solution deposition (Lei 2008), non-reversible galvanic cell method (Bi 2008), microwave radiation-assisted chelating agent method (Sun 2011) and precipitation technique (Choi 2010, Xing 2011). However, these methods generally require expensive and sophisticated equipments, high temperature calcinations, prolonged annealing etc. But most of the above methods results in poor phase purity, low yield and high consumption of time and energy. A possible alternative to encounter these factors, a novel modified auto-igniting combustion process is employed (Thomas 2010, Vidya 2011). This method involves single step combustion of precursor solution without any intermediate calcinations steps. Phase pure ultra fine nano powder can be obtained at very low temperature through this method.

Therefore, in the present paper, we report for the first time, the synthesis of phase pure nanocrystalline scheelite type  $\text{SrMoO}_4$  using the modified combustion technique and sintered at a relatively low temperature with high sintered density. Its structural, particulate, optical, morphological and dielectric properties are studied. A detailed study on the optical behaviour of the nano powder was also done and the results are correlated with vibrational spectroscopic studies. The application of material as low temperature co-fired ceramics (LTCC) is also discussed.

## 2. Experimental

Preliminary step of combustion synthesis is the preparation of a precursor solution containing strontium and molybdenum ions. Aqueous solutions containing strontium and molybdenum ions were prepared from stoichiometric amounts of Strontium nitrate ( $\text{Sr}(\text{NO}_3)_2$ , Alfa Aesa, 99.99%) dissolved in double distilled water and Molybdenum trioxide ( $\text{MoO}_3$ , CDH, 99.5%) dissolved in 10% ammonia solution. Citric acid was added as a complexing agent. Amount of citric acid was calculated based on total valence of the oxidizing and reducing agents for maximum release of energy during combustion. Oxidant to fuel ratio of the system was adjusted by adding concentrated nitric acid and ammonium hydroxide and the ratio was kept at unity. The solution containing the precursor mixture at a pH of  $\sim 7.0$  was stirred well for uniform mixing and obtained a clear solution with no precipitate or sedimentation. This precursor solution was heated on a hot plate at about  $250^\circ\text{C}$  in a ventilated fume hood. The solution boils on heating and undergoes dehydration leading to smooth deflation accompanied by foam. The foam ignited by itself on further heating giving voluminous and fluffy product of combustion. Fine nano powder of  $\text{SrMoO}_4$  with a pale green colour thus obtained is used for further characterization.

The structure and phase purity of the powder was examined by powder X-ray diffraction technique using X-ray diffractometer (Model. Philips Expert Pro) using  $\text{CuK}_\alpha$  radiation. The investigation of morphology was examined using transmission electron microscopy (TEM, Model-Hitachi H-600 Japan) operating at 200 kV. The samples for Transmission Electron Microscope (TEM) were prepared by ultrasonically dispersing the powder in methanol and allowing a drop of this to dry on a carbon-coated copper grid. Raman and FT-IR spectra of the sample were also recorded. Raman spectra was obtained using Bruker RFS100/S spectrometer with a resolution of  $4\text{ cm}^{-1}$  from  $50$  to  $1000\text{ cm}^{-1}$  using Nd:YAG laser source, lasing at  $1064\text{ nm}$  and power  $150\text{ mW}$  and by a germanium diode detector. The Infrared (IR) spectra of the samples were recorded in the range  $400\text{--}4000\text{ cm}^{-1}$  on a

Thermo-Nicolet Avatar 370 Fourier Transform Infrared (FTIR) Spectrometer using KBr pellet method. The photoluminescence spectrum of the sample was measured using Fluorolog@-3 Spectrofluorometer. The photons from the source were filtered by an excitation spectrometer. The monochromatic radiation was then allowed to fall on the disc samples and the resulting radiation was filtered by an emission spectrometer and then fed to a photomultiplier detector. The variation of intensity was recorded as a function of wavelength. The absorption spectra were taken using a Jasco UV-Visible spectrophotometer in the wavelength range 200-800 nm.

To study the sintering behavior of the nanoparticles obtained by the present combustion method, the as-prepared SrMoO<sub>4</sub> nanoparticles were mixed with 5% polyvinyl alcohol and pressed in the form of a cylindrical pellet with 12 mm diameter and 2 mm thickness at a pressure of about 350 MPa using a hydraulic press. The pellet was then sintered at 850°C for 2 h and the sintered density, calculated by the Archimedes method. Polished samples were thermally etched at 800°C and were used for scanning electron microscopy (SEM, JEOL JSM 5610 LV). The dielectric properties of the samples were measured in the radio frequency region using LCR meter (Hioki-3532-50) for the frequency range 100 Hz –5 MHz in the temperature range 50-250°C.

### 3. Results and discussion

#### 3.1 Structure determination

The structure of the as prepared nano a powder of SrMoO<sub>4</sub> was characterized by X-ray diffraction (XRD) technique and the pattern is shown in Fig. 1. All the diffraction peaks can be indexed for a scheelite-type tetragonal structure with space group I41/a. The sharp and intense peaks indicate that the powders are well crystallized. The obtained lattice parameters were  $a = b = 5.3796 \text{ \AA}$  and  $c = 11.9897 \text{ \AA}$ , with volume unit cell of  $346.9920 \text{ \AA}^3$ . These values are in agreement with the reported data in the respective JCPDS card No 85-0586. The crystallite size corresponding to maximum reflection (112) estimated by the Scherer formulae is 20 nm. No extra peaks corresponding to any

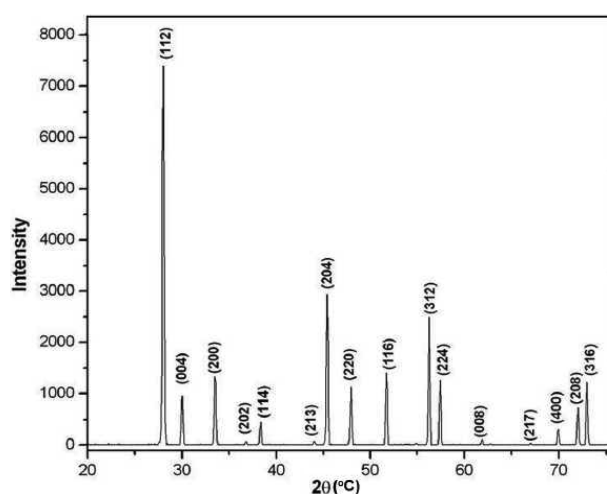


Fig. 1 XRD pattern of as prepared nano SrMoO<sub>4</sub>

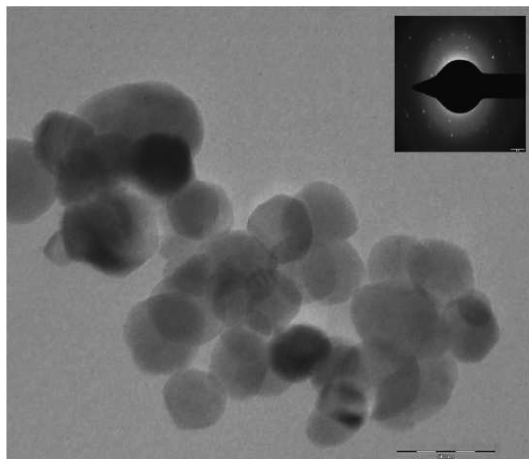


Fig. 2 TEM image of nano SrMoO<sub>4</sub>

other impurity or additional phase is present. Thus it can be inferred that the molybdenum atoms coordinated with four oxygen atoms and the strontium atoms coordinated with eight oxygen atoms to form the unit cell of SrMoO<sub>4</sub> (Marques 2010).

The investigation of morphology of nanocrystalline SrMoO<sub>4</sub> powders are examined using TEM images. Fig. 2 shows the TEM image of as prepared nano SrMoO<sub>4</sub>. The average particle size calculated from the TEM micrograph is 18 nm. The particle shows homogeneous morphology with a little agglomeration which indicates that the sample possesses excellent nano nature. In this micrograph, the dark areas are related to the high concentration of aggregated crystals, confirming also that these structures are not internally hollow. Inset of Fig. 2 shows selected area electron diffraction (SAED) pattern of SrMoO<sub>4</sub>. SAED patterns are composed of a number of bright spots arranged into concentric rings. The SAED performed on the nanocrystals presented common electron diffraction patterns of polycrystalline materials, as a consequence of the aggregated nature. The electrons have been reflected and diffracted from crystallographic planes of the unit cells belonging to the products to produce bright spots. The rings are diffuse and hollow showing that the products are composed of nanocrystals with different orientations (Cavalcante 2012). This is indicative of the polycrystalline nature of the crystallites, but the spotty nature of the SAED pattern can be due to the fact that the finer crystallites having related orientations are agglomerated together resulting in a limited set of orientations.

The structure is all over again close examined by means of vibrational analysis. Scheelite type crystal with space group I41/a space group with two formula units per primitive cell. The compound SrMoO<sub>4</sub> has [MoO<sub>4</sub>]<sup>2-</sup> molecular ionic units with strong Mo-O covalent bonds, which have weak coupling with Sr<sup>2+</sup> cations. The  $T_d$  symmetry of the five tetrahedral MoO<sub>4</sub> ions is reduced to  $S_4$  in the crystal lattice and the presence of two MoO<sub>4</sub> reduces to the point-group symmetry  $C_{4h}$ . Group theoretical calculation shows that the vibrational degrees of freedom of SrMoO<sub>4</sub>, excluding the three acoustical modes ( $A_u + E_u$ ) can be written as

$$\Gamma = 3A_g + 4A_u + 5B_g + 3B_u + 5E_g + 4E_u$$

All the even vibrations  $3A_g$ ,  $5B_g$  and  $5E_g$  are Raman active and the odd modes  $4A_u$  and  $4E_u$  are IR active. The  $3B_u$  modes are neither Raman nor IR active.

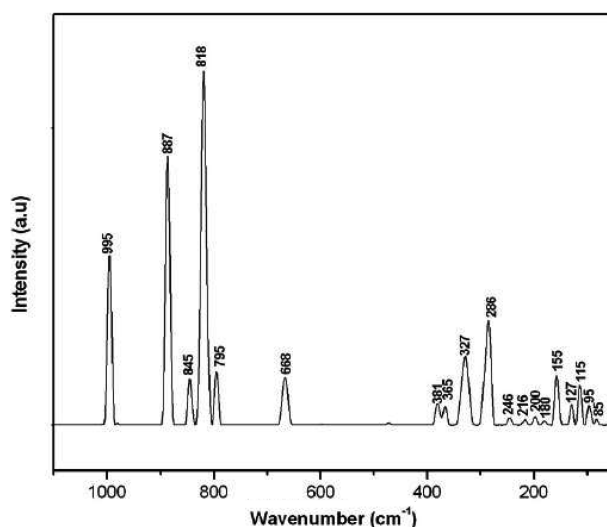


Fig. 3 Raman spectra of nano SrMoO<sub>4</sub>

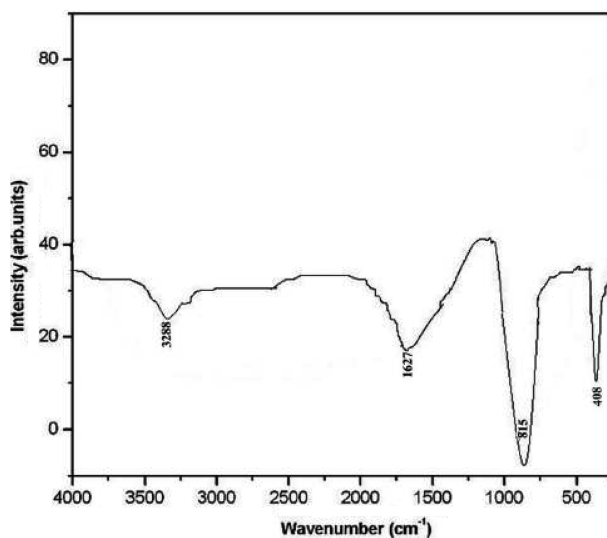


Fig. 4 FT-IR spectra of nano SrMoO<sub>4</sub>

The Raman and IR spectra of SrMoO<sub>4</sub> obtained are shown in the Figs. 3 and 4. The Raman spectrum of the as prepared sample obtained in the present study matches exactly with those reported early (Christofilos 1995), except for three intense bands at 818, 688 and 286 cm<sup>-1</sup>. These bands are identified as the Raman active modes  $\nu_1 A_{1g}$ ,  $\nu_2 E_g$  and  $\nu_5 F_{2g}$  modes respectively of MoO<sub>6</sub> octahedron due to the presence of SrMoO<sub>3</sub> formed along with the expected phase SrMoO<sub>4</sub>, during the combustion process. Thus from Raman spectra the presence trace amount SrMoO<sub>3</sub> phase is detected which is not observed in the XRD pattern.

The 13 remaining Raman active modes  $3A_g$ ,  $5B_g$  and  $5E_u$  can be divided into two groups. The internal modes observed in the region 887-180 cm<sup>-1</sup> and the external modes observed in the region

155-95  $\text{cm}^{-1}$ . The internal modes include the vibrational and rotational modes of the tetrahedron, with latter occurring towards the 4 lower frequency regions of internal modes. The  $A_g$  modes are observed at 887, 327 and 180  $\text{cm}^{-1}$  and the three  $B_g$  modes at 845, 365 and 327  $\text{cm}^{-1}$ , the bands at 327  $\text{cm}^{-1}$  is the superposition of  $\nu_2 A_g$  and  $\nu_2 B_g$  modes of vibrations the three  $E_g$  internal modes are observed at 795, 381 and 286  $\text{cm}^{-1}$ . The modes involving the free rotation in the limiting case of the uncoupled  $\text{MoO}_4$  ions are observed at 246 and 180  $\text{cm}^{-1}$  which have the  $E_g$  and  $A_g$  symmetries, respectively. The external modes involve the movement of  $\text{MoO}_4$  ions as a whole which are only weakly coupled. Hence the 4 external modes  $2B_g$  and  $2E_g$  are assigned to the lowest frequency bands. The very weak bands at 216 and 200  $\text{cm}^{-1}$  may be due to the Raman inactive  $A_u$  and  $E_u$  modes.

The IR spectrum shows a very strong absorption band at 815  $\text{cm}^{-1}$  and a strong one at 408  $\text{cm}^{-1}$ . The former is due to the strong Mo-O stretch vibration mode and the latter is due to the weak Mo-O bending vibration. These correspond to the IR active  $\nu_3 A_u$  and  $\nu_4 A_u$  modes of vibrations. Also the respective bands at 3288 and 1627  $\text{cm}^{-1}$  can be ascribed to O-H stretching vibration and H-O-H bending vibration of physically adsorbed water on the sample surface.

### 3.2 Optical properties

The PL emission spectra of as prepared  $\text{SrMoO}_4$  and sample annealed at 700°C for 1 h at an excitation 420 nm are shown in the Figs. 5 and 6 respectively. The emission spectra show two intense peaks, one ascribed to red-yellow region and other in the green region. On comparing the PL spectra of as prepared sample with the sample heated at 700°C given in Fig. 6 it is very clear that green emission intensity increases and that of red-yellow region decreases. Also the green

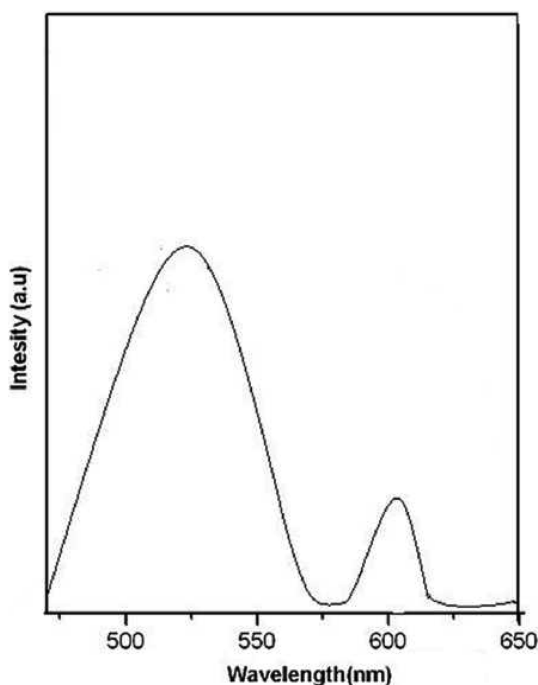


Fig. 5 PL emission spectra of as prepared nano  $\text{SrMoO}_4$

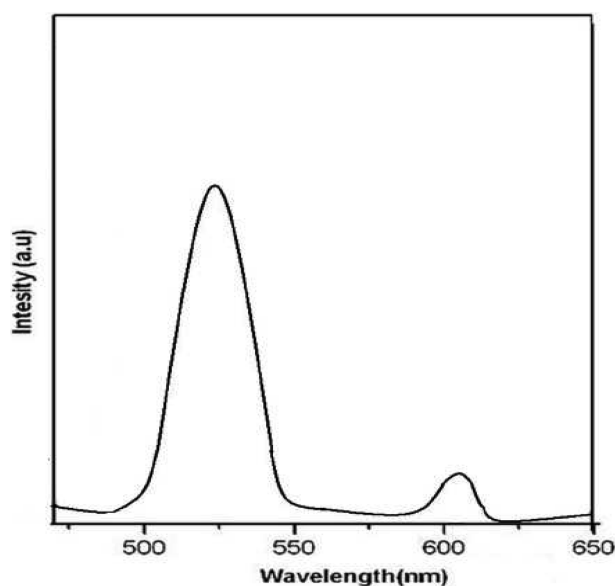


Fig. 6 PL emission spectra of nano SrMoO<sub>4</sub> heated at 700°C

emission becomes sharp compared to the broad emission peak in the Fig. 5. The difference observed in the position of the maximum PL emission is probably associated with the structural organization levels and thermal treatment conditions. Many valid hypotheses are put forward in the literature to explain the possible mechanisms responsible for the emission process of the SrMoO<sub>4</sub> (Marques 2006, Sczancoski 2008).

The components of the PL emission bands are probably linked to specific atomic arrangements. In the case of scheelite-type materials the PL emission is related to the structural disorder in MoO<sub>4</sub>. During the polyesterification stage of the citrate solution containing the molybdenum and strontium ions, a structural transformations from disordered to ordered phases occurs (Marques 2005, Santos 2011). Ideally molybdenum has a tendency to bond with four oxygen atoms but before it reaches this ideal configuration it has various co-ordination numbers possible. Thus before the crystallization, the structure is a mixture of MoO<sub>x</sub> clusters. This mixture of the clusters is regarded as the source of the PL in the red region. When the perfect crystallization is reached, only MoO<sub>4</sub> clusters exist, the PL in the red region practically vanishes and the PL in the green intensifies. The MoO<sub>4</sub> unit is responsible for the green luminescence of molybdates. From the Raman studies the presence of distorted octahedron MoO<sub>6</sub> due to the presence of trace amount of SrMoO<sub>3</sub> along with the main phase SrMoO<sub>4</sub> is noted thus the sample can be thought of as a mixture of MoO<sub>6</sub>-MoO<sub>4</sub> clusters. The broad PL emission band of as prepared sample also points to the fact that the emission process is a multiphonon process, that is, a system in which relaxation occurs by various paths, involving the participation of numerous states (Santos 2011). These numerous states are formed due to the structural disorder in the MoO<sub>4</sub> and distorted MoO<sub>6</sub> unit. In short, MoO<sub>4</sub> clusters are responsible for green luminescence and red-yellow emission is due to MoO<sub>6</sub>-MoO<sub>4</sub> clusters. Chen and Gao (Chen 2007) argued that the green emission is a result of the intrinsic luminescent behavior of the MoO<sub>4</sub><sup>2-</sup> group. The authors also mentioned that the transition of the green luminescence is due 3T<sub>1</sub>, 3T<sub>2</sub>\_1A<sub>1</sub> transition in the tetrahedral molybdates group.

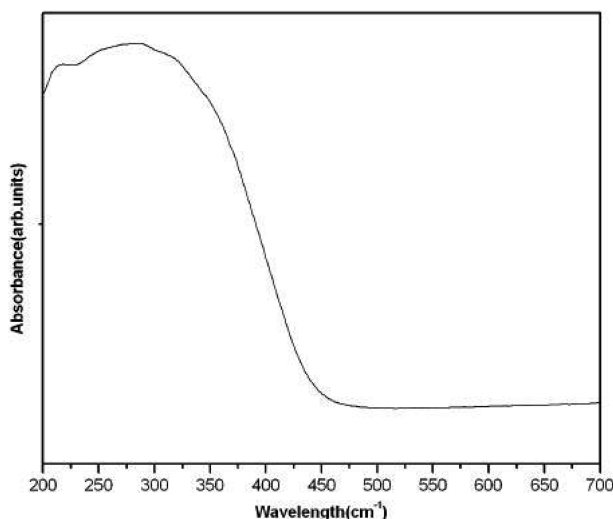


Fig. 7 UV-Vis absorption spectrum of SrMoO<sub>4</sub> nanocrystals

The overall PL emission spectra indicate that the fraction of overall PL emission ascribed to the red emission band increases with the degree of structural disorder. In the most crystalline structure, the fraction of the green emission band is bigger than that of the red emission band. The nano powder heat treated at 700°C display the biggest green area because it is a completely ordered structure and is similar to the reports of Marques *et al.* (Marques 2005). Thus PL is directly linked to the order-disorder of the material which was evidently confirmed by vibrational analysis. Thus the PL spectra show that the transition from a short range disordered structure to a completely ordered structure takes place due to heat treatment. The completely disordered structure is suitable for a good PL emission in the red region and that a complete ordered structure is suitable for a good PL emission in the green region.

The UV absorption spectrum of the sample is shown in the Fig. 7. The absorption spectrum is broad with a maximum peak at 275 nm extending to blue region of visible spectrum. From the absorption spectra it is clear that sample absorbs heavily within the UV region but moderately in the visible region. Such materials found applications in filters and sensors for UV radiation. The absorption spectrum of SrMoO<sub>4</sub> exhibits typical optical behavior of a wide-band gap semiconductor. The optical absorption in the wavelength region shorter than 400 nm is mainly attributed to the electron transition from the top of the valence band to the bottom of the conduction band. Also there is a small degree of visible attenuation around 455 nm gives the sample a slight pale greenish-yellow colour which is the complementary colour of indigo.

A material can be characterized by the estimation of its band gap energy, which is the energy difference between valence band and conduction band. The equation proposed by Wood and Tauc (Tauc 1968, Charles 1989) was used to estimate the optical band gap. According to these authors, the optical band gap energy is related with absorbance and photon energy by equation,

$$(\alpha h\nu) = B(h\nu - E_g)^m$$

where  $\alpha$  is the absorbance,  $h$  is the Planck constant,  $\nu$  is the frequency and  $E_g$  is the optical band gap.

Values of  $m$  for allowed direct and non-direct transitions are 1/2 and 2, respectively.

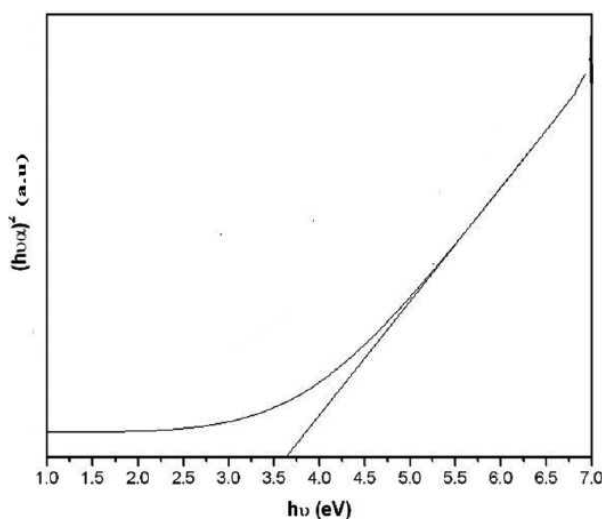


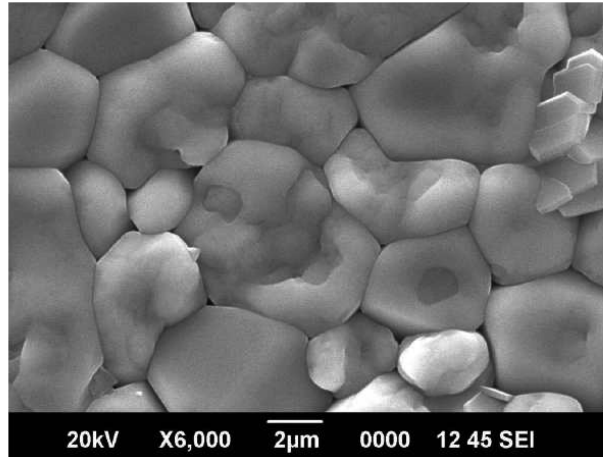
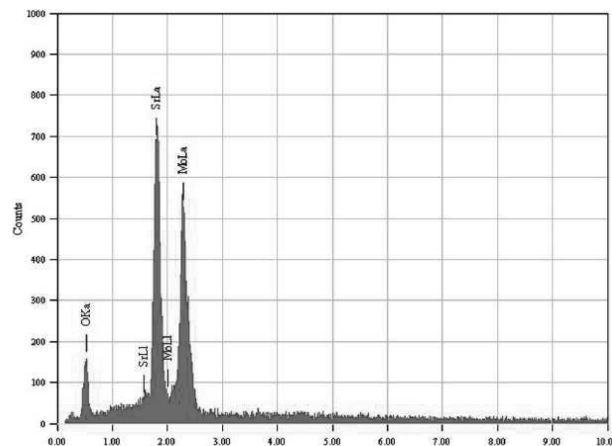
Fig. 8 Tauc's plot of the optical absorption spectrum of SrMoO<sub>4</sub> nanopowder

The band gap in the materials is related with absorbance and photon energy. Fig. 8 shows a Tauc's plot of the optical absorption spectrum of SrMoO<sub>4</sub> nano powder. The indirect optical energy gap can be obtained from the intercept of the resulting linear region with the energy axis at  $(\alpha h\nu)^2 = 0$ . Thus determined optical band gap value of SrMoO<sub>4</sub> is approached to 3.7 eV. This experimentally obtained band gap is found to be slightly less than the early reported ones (Sczancoski 2008, Thongtem 2010). In fact, energy band gap depends on several factors such as the electro negativity of transition metal ions, connectivity of the polyhedrons and deviation in the O–X–O bonds, distortion of the  $[\text{XO}_4]^{2-}$  tetrahedrons, growth mechanism and degree of structural order– disorder in the lattice. In the present case decrease in band gap can be attributed to the presence of MoO<sub>3</sub> cluster which is present along with MoO<sub>4</sub>. This might have resulted in the formation of intermediate energy levels in between the actual ones which resulted in the decrease of band gap energy (Cavalcante 2008, Sczancoski 2009, Almeida 2012).

### 3.3 Sintering and dielectric property

The sintering behavior of the nano crystals of SrMoO<sub>4</sub> powder synthesized through the present combustion route was studied. The relative green density of the specimen used for the sintering study was 55%. A sintered density of ~95% of the theoretical value was obtained upon sintering the compacted specimen at 850°C for 2 h without using any sintering aid. It may be noted that for SrMoO<sub>4</sub> powder prepared through solid state reaction method by earlier workers, the green pellet had to be heated at a temperature of 1050°C to obtain a well sintered pellet (Choi 2007). The sintering temperature of our sample is nearly 200°C less than that reported for bulk powder. The high sintered density of SrMoO<sub>4</sub> ceramic obtained at relatively short duration of sintering can be attributed to the ultra fine nature of the SrMoO<sub>4</sub> nano powder used in the present study.

The scanning electron microscopic (SEM) studies on the sintered sample are shown in Fig. 9. The surface morphology of sintered sample shows maximum densification. It is observed from the micrograph that the agglomerates of the as-prepared nano powder that the size of the grains have

Fig. 9 SEM micrograph of sintered SrMoO<sub>4</sub>Fig. 10 EDAX spectrum of SrMoO<sub>4</sub>

increased from 500 nm to about 2  $\mu\text{m}$  due to sintering, with no cracks and with very little porosity. The EDAX pattern of the sintered sample is given in Fig. 10. The EDAX analysis shows that all the elements such as strontium, molybdenum and oxygen are present in the sample in the same stoichiometric concentrations and no other impure matter is present. As the sintering temperature of nano SrMoO<sub>4</sub> is 850°C, it comes under the category of low temperature co-fired ceramics (LTCC) materials.

The dielectric property of a particular material determines its functionality. The variation of dielectric constant and loss factor in the frequency range 100 Hz to 5 MHz is given in the Fig. 11. It can be clearly noted that loss factor decreases as frequency increases while the dielectric constant remains almost unaltered at higher frequencies. The dielectric constant  $\epsilon_r$  and loss factor at 5 MHz is 9.50 and  $7.5 \times 10^{-3}$  respectively. The value of dielectric constant is nearly same as that reported for the SrMoO<sub>4</sub> conventional powder (Choi 2007). LTCC materials with low  $\epsilon_r$  are suitable for substrate application.

The low loss and low dielectric constant makes SrMoO<sub>4</sub> a potential candidate for substrate applications and as electronic packing materials. The variation of dielectric constant and loss factor

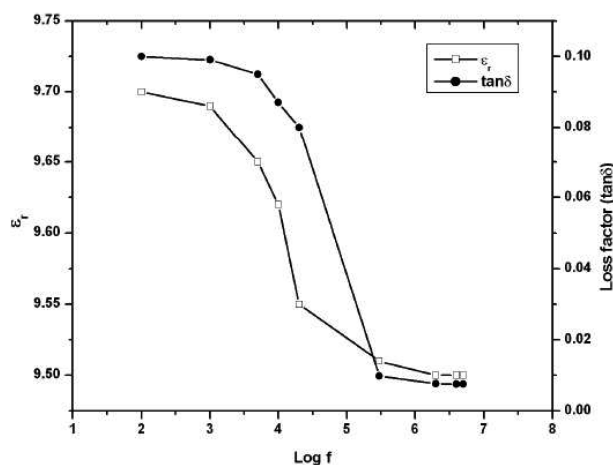


Fig. 11 Variation of dielectric constant and loss factor with frequency

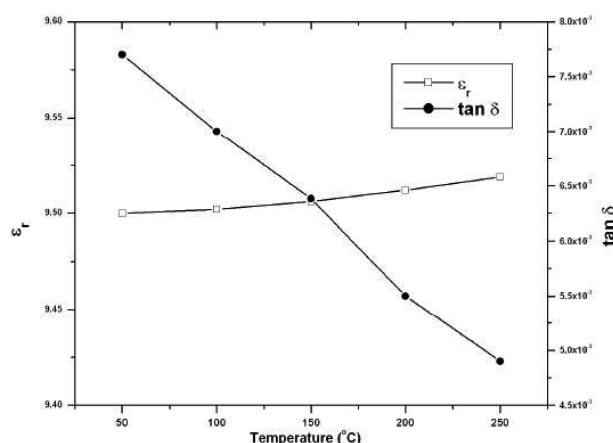


Fig. 12 Variation of dielectric constant and loss factor with temperature

with temperature is given in the Fig. 12. It is clear from the graph that the temperature dependence of dielectric constant is very minimal in the measured temperature range. The loss factor further lowers with increase of temperature and is of order 10<sup>-3</sup> at temperature above 200°C. The dielectric constant ε<sub>r</sub> values of the SrMoO<sub>4</sub> pellets at 5 MHz in room temperature were 9.51 and 4.9 × 10<sup>-3</sup> respectively. From the graph we can see that dielectric constant remains almost unaltered with temperature variation while loss factor decreases as temperature increases. Thus nano SrMoO<sub>4</sub> is suitable material for temperature sensitive applications.

#### 4. Conclusions

In summary, nanocrystalline SrMoO<sub>4</sub> powders were prepared through combustion synthesis. The sample posses tetragonal structure with lattice constant  $a = b = 5.3796 \text{ \AA}$  and  $c = 11.9897 \text{ \AA}$ . Particle

size obtained from TEM micrograph is 18 nm. From the vibrational analysis peaks corresponding to scheelite structure were assigned. Raman spectra show the presence of trace amount of SrMoO<sub>4</sub> along with the expected main phase. SrMoO<sub>4</sub> is an excellent luminescent material with two peaks one in green region and other in red region which indicates the presence of both MoO<sub>4</sub> and MoO<sub>3</sub> clusters, respectively. On annealing the disordered MoO<sub>3</sub> transforms to ordered MoO<sub>4</sub> clusters. The optical band gap determined from the UV-V is absorption spectra is found to be nearly 3.7 eV. Nano SrMoO<sub>4</sub> was sintered at 850°C which is much less than that of the conventional sample. SEM micrograph of the sintered sample shows that sample has achieved maximum densification. The dielectric constant of nano SrMoO<sub>4</sub> is found to be 9.50 and loss factor is  $7.5 \times 10^{-3}$  at 5 MHz. The dielectric constant remains unaffected while loss decreases with rise of temperature. The low sintering temperature, dielectric constant and loss makes nano SrMoO<sub>4</sub> an excellent low temperature co-fired ceramics (LTCC) in addition to good a luminescent material.

## References

- Angloher, G., Bucci, C., Cozzini, C., Feilitzsch, F., Frank, T., Hauff, D., Henry, S., Jagemann, Th., Jochum, J., Kraus, H., Majorovits, B., Ninkovic, J. and Petricca, F. (2004), "Nucl. Cresst-II: dark matter search with scintillating absorbers", *Instrum. Meth. Phys. Res. A.*, **520**(1-3), 108-111.
- Almeida, M.A.P., Cavalcante, L.S., M., Siu Li, Varela, J.A. and Longo, E. (2012), "Structural refinement and photoluminescence properties of MnWO<sub>4</sub> nanorods obtained by microwave-hydrothermal synthesis", *J. Inorg. Organomet. P.*, **22**(1), 264-271.
- Basiev, T.T., Sobol, A.A., Voronko, Y.K. and Zverev, P.G. (2000), "Spontaneous raman spectroscopy of tungstate and molybdate crystals for raman lasers", *Opt. Mater.*, **15**(3), 205-216.
- Bi, J., Cui, C.H., Lai, X., Shi, F. and Jiang, D. (2008), "Synthesis of luminescent SrMoO<sub>4</sub> thin films by a non-reversible galvanic cell method", *Mater. Res. Bull.*, **43**(4), 743-747.
- Bi, J., Wu, L., Zhang, Y., Li, Z., Li, J. and Fu, X. (2009), "Solvothermal preparation, electronic structure and photocatalytic properties of PbMoO<sub>4</sub> and SrMoO<sub>4</sub>", *Appl. Catal. B-Environ.*, **91**(1-2), 135-143.
- Cavalcante, L.S., Longo, V.M., Sczancoski, J.C., Almeida, M.A.P., Batista, A.A., Varela, J.A., Orlandi, M.O., Longo, E. and Siu Li, M. (2012), "Electronic structure, growth mechanism and photoluminescence of CaWO<sub>4</sub> crystals", *Cryst. Eng. Comm.*, **14**(3), 853-868.
- Cavalcante, L.S., Sczancoski, J.C., Tranquilin, R.L., Joya, M.R., Pizani, P.S., Varela, J.A. and Longo, E. (2008), "BaMoO<sub>4</sub> powders processed in domestic microwave-hydrothermal: Synthesis, characterization and photoluminescence at room temperature", *J. Phys. Chem. Solids*, **69**(11), 2674-2680.
- Chang, I.C., Katzka, P., Jacob, J. and Estrin, S. (1996), "Programmable acousto-optic filter", *IEEE Ultrason. Symp.*, **2**, 819-825.
- Charles, M.W., Nick Jr, H. and Gregory, E.S. (1989), *Physical properties of semiconductors*, Prentice-Hall, Englewood Cliffs, NJ.
- Chen, L. and Gao, Y. (2007), "Mechanisms and applications of cell electrochemical technique to prepare luminescent SrMoO<sub>4</sub> thin films", *J. Chem. Eng.*, **131**(1-3), 181-185.
- Cheng, Y., Wang, Y.S., Chen, D. and Bao, F. (2005), "Evolution of single crystalline dendrites from nanoparticles through oriented attachment", *J. Phys. Chem. B.*, **109**(2), 794-798.
- Choi, E.J. and Huh, Y.D. (2010), "Morphological evolution of SrMoO<sub>4</sub> crystals from wires to notched spheres through oriented attachment", *B. Kor. Chem. Soc.*, **31**(1), 196-198.
- Christofilos, D., Kourouklis, G.A. and Ves, S. (1995), "A high pressure raman study of calcium molybdate", *J. Phys. Chem. Solids.*, **56**(8), 1125-1129.
- Geun-Kyu Choi, Jeong-Ryeol Kim, Sung-Hun Yoon and Kug-Sun Hong (2007), "Microwave dielectric properties of scheelite (A = Ca, Sr, Ba) and wolframite (A = Mg, Zn, Mn) AMoO<sub>4</sub> compounds", *J. Eur. Ceram. Soc.*, **27**(8-9), 3063-3067.
- Harris, S.E. and Nieh, S.T.K. (1970), "CaMoO<sub>4</sub> electronically tunable. optical filter", *Appl. Phys. Lett.*, **17**, 223-225.

- Ishii, M. and Kobayashi, M. (1991), "Single crystals for radiation detectors", *Prog. Cryst. Growth Ch.*, **23**, 245-311.
- Jia, G.H., Tu, C.Y., You, Z.Y., Li, J.F., Zhu, Z.J., Wang, Y. and Wu, B.C. (2004), "Czochralski technique growth of pure and rare-earth-doped SrWO<sub>4</sub> crystals", *J. Cryst. Growth.*, **273**(1-2), 220-225.
- Lei, H., Zhu, X., Sun, Y. and Song, W. (2008), "Preparation of SrMoO<sub>4</sub> thin films on Si substrates by chemical solution deposition", *J. Cryst. Growth.*, **310**(4), 789-793.
- Marques, A.P.A., de Melo, D.M.A., Longo, E., Paskocimas, C.A., Pizani, P.S. and Leite, E.R. (2005), "Photoluminescence properties of BaMoO<sub>4</sub> amorphous thin films", *J. Solid. State Chem.*, **178**(7), 2346-2353.
- Marques, A.P.A., De Melo, D.M.A., Paskocimas, C.A., Pizani, P.S., Joya, M.R., Leite, E.R. and Longo, E. (2006), "Photoluminescent BaMoO<sub>4</sub> nanopowders prepared by complex polymerization method (CPM)", *J. Solid. State. Chem.*, **179**(3), 671-678.
- Marques, V.S., Cavalcante, L.S., Sczancoski, J.C., Alcantara, A.F.P., Orlandi, M.O., Moraes, E., Longo, E., Varela, J.A., Siu, Li M. and Santos, M.R.M.C. (2010), "Effect of different solvent ratios (water/ethylene glycol) on the growth process of CaMoO<sub>4</sub> crystals and their optical properties", *Cryst. Growth Des.*, **10**(11), 4752-4768.
- Paski, E.F. and Blades, M.W. (1988), "Analysis of inorganic powders by time-wavelength resolved luminescence spectroscopy", *Anal. Chem.*, **60**(11), 1224-1230.
- Ryu, J.H., Yoon, J.W., Lim, C.S., Oh, W.C. and Shim, K.B. (2005), "Microwave-assisted synthesis of CaMoO<sub>4</sub> nano-powders by a citrate complex method and its photoluminescence property", *J. Alloy Compd.*, **390**(1-2), 245-249.
- Sabharwal, S., Sangeeta, C. and Desai, D.G. (2006), "Investigations of single crystal growth of PbMoO<sub>4</sub>", *Cryst. Growth Des.*, **6**(1), 58-62.
- Santos, M.A., Picon, F.C., Alves, C.N., Pizani, P.S., Varela, J.A. and Longo, E. (2011), "The role of short-range disorder in BaWO<sub>4</sub> crystals in the intense green photoluminescence", *J. Phys. Chem. C*, **115**(24), 12180-12186.
- Sczancoski, J.C., Bomio, M.D.R., Cavalcante, L.S., Joya, M.R., Pizani, P.S., Varela, J.A., Longo, E., Siu Li, M. and Andrés, J.A. (2009), "Morphology and blue photoluminescence emission of PbMoO<sub>4</sub> processed in conventional hydrothermal", *J. Phys. Chem. C.*, **113**(14), 5812-5822.
- Sczancoski, J.C., Cavalcante, L.S., Joya, M.R., Espinosa, J.W.M., Pizani, P.S., Varela, J.A. and Longo, E. (2009), "Synthesis, growth process and photoluminescence properties of SrWO<sub>4</sub> powders", *J. Colloid Interf. Sci.*, **330**(1), 227-236.
- Sczancoski, J.C., Cavalcante, L.S., Joya, M.R., Varela, J.A., Pizani, P.S. and Longo, E. (2008), "SrMoO<sub>4</sub> powders processed in microwave-hydrothermal: Synthesis, characterization and optical properties", *Chem. Eng. J.*, **140**(1-3), 632-637.
- Sczancoski, J.C., Cavalcante, L.S., Marana, N.L., da Silva, R.O., Tranquilin, R.L., Joya, M.R., Pizani, P.S., Varela, J.A., Sambrano, J.R., Siu Li, M., Longo, E. and Andrése, J. (2010), "Electronic structure and optical properties of BaMoO<sub>4</sub> powders", *Curr. Appl. Phys.*, **10**(2), 614-624.
- Streifer, W. and Saltz, P. (1973), "Transient analysis of an electronically tunable dye laser - 2. Analytic study", *IEEE J. Quantum Elect.*, **9**(6), 563-569.
- Sun, Y., Li, C., Wang, L., Ma, X., Zhang, Z., Song, M. and Ma, P. (2011), "Synthesis of SrMoO<sub>4</sub> microstructures by the microwave radiation-assisted chelating agent method", *Cryst. Res. Technol.*, **46**(9), 973-978.
- Tauc, J. (1968), "Optical properties and electronic structure of amorphous Ge and Si", *Mater. Res. Bull.*, **3**(1), 37-46.
- Thomas, J.K., Padma Kumar, H., Solomon, S., Mathai, K.C. and Koshy, J. (2010), "Nanocrystalline SrHfO<sub>3</sub> synthesized through a single step auto-igniting combustion technique and its characterization", *J. Alloy. Compd.*, **508**(2), 532-535.
- Thongtem, T., Kungwankunakorn, S., Kuntalue, B., Phuruangrat, A. and Thongtem, S. (2010), "Luminescence and absorbance of highly crystalline CaMoO<sub>4</sub>, SrMoO<sub>4</sub>, CaWO<sub>4</sub> and SrWO<sub>4</sub> nanoparticles synthesized by coprecipitation method at room temperature", *J. Alloy. Compd.*, **506**(1), 475-481.
- Thongtem, T., Phuruangrat, A. and Thongtem, S. (2008), "Characterization of MMoO<sub>4</sub> (M = Ba, Sr and Ca) with different morphologies prepared using a cyclic microwave radiation", *Mater. Lett.*, **62**(3), 454-457.
- Vidya, S., Rejith, P., John, A., Solomon, S., Deepa, A.S. and Thomas, J.K. (2011), "Electrical, optical and

- vibrational characteristics of nano structured yttrium barium stannous oxide synthesized through a modified combustion method”, *Mater. Res. Bull.*, **46**(10), 1723-1728.
- Xing, G., Li, Y., Li, Y., Wu, Z., Sun, P., Wang, Y., Zhao, C. and Wu, G. (2011), “Morphologycontrollable synthesis of SrMoO<sub>4</sub> hierarchical crystallites via a simple precipitation method”, *Mater. chem. Phys.*, **127**(3), 465-470.
- Yang, P., Yao, G.Q. and Lin, J.H. (2004), “Photoluminescence and combustion synthesis of CaMoO<sub>4</sub> doped with Pb<sup>2+</sup> Inorg”, *Chem. Commun.*, **7**(3), 389-391.
- Yu, H., Li, Z., Lee, A.J., Li, J., Zhang, H., Wang, J., Pask, H.M., Piper, J.A. and Jiang, M. (2011), “A continuous wave SrMoO<sub>4</sub> Raman laser”, *Opt. Lett.*, **36**(4), 579-581.
- Zeng, H.C. (1997), “Correlation of PbMoO<sub>4</sub> crystal imperfections to Czochralski growth process”, *J. Cryst. Growth.*, **171**(3-4), 136-145.
- Zhang, Y., Yang, F., Yang, J., Tang, Y. and Yuan, P. (2005), “Synthesis of crystalline SrMoO<sub>4</sub> nanowires from polyoxometalates”, *Solid. State. Commun.*, **133**(12), 759-763.
- Zverev, P.G. (2004), “Vibronic relaxation of raman modes in CaMoO<sub>4</sub> and PbMoO<sub>4</sub> molecular ionic crystals”, *Phys. Status Solidi C.*, **1**(11), 3101-3105.